内インスリンシグナルの障害を介してアルツハイマー病脳内病態を修飾する」第10回日本抗加齢医学会総会、2010年6月12日、京都(口頭)

12. 武田 朱公、里 直行、内尾 こずえ、澤田 京子、國枝 孝典、篠原 充、楽木 宏実、森下 竜一「糖負荷による血中Aβの変動を利用した新たなアルツハイマー病診断指標の探索：全身糖代謝が血中Aβ濃度に与える影響の検討」第10回日本抗加齢医学会総会、2010年6月12日、京都(ポスター)

13. 武田 朱公、里 直行、内尾-山田 こずえ、楽木 宏実、森下 竜一「糖尿病とアルツハイマー病の相互的病態修飾機序の解明：糖尿病合併アルツハイマー病モデルマウスの作成とその病態解析」第57回日本実験動物学会総会、2010年5月12日、京都(口頭)

14. Takeda S, Sato N, Uchio-Yamada K, Rakugi H, Morishita R. Diabetes Accelerated Memory Dysfunction via Cerebrovascular Inflammation and Beta-Amyloid Deposition in Alzheimer Mouse Model: Generation of Novel Transgenic Mouse Models of Alzheimer Disease with Diabetes. Vascular Consequences of Obesity and Insulin Resistance-Pathobiology and Pharmacology, 23rd Scientific Meeting of the International Society of Hypertension (ISH2010), Vancouver, Canada (September 27, 2010)(口頭)

15. Takeda S, Sato N, Uchio-Yamada K, Sawada K, Kunieda T, Shinohara M, Rakugi H, Morishita R. Diabetes mellitus exacerbated learning impairment via cerebrovascular inflammation and disturbance of brain insulin signaling in Alzheimer mouse models with diabetes. Alzheimer's Association International Conference on Alzheimer Disease 2010 (ICAD2010), Honolulu, Hawaii (July 12, 2010)(ポスター)

図１　実験群

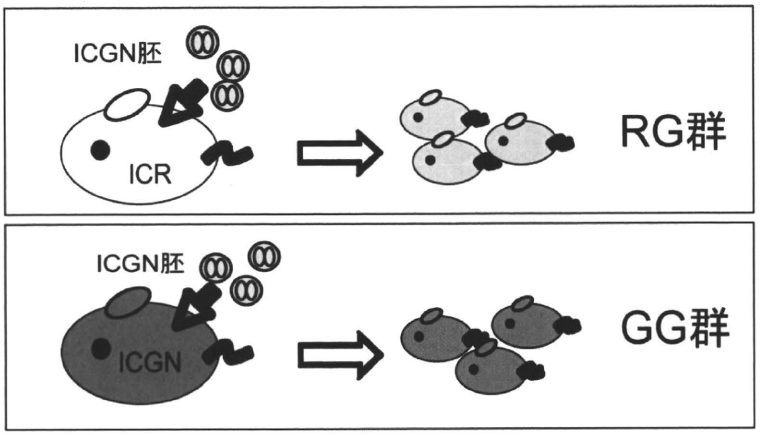


表１

| | RG | | GG | |
|---|---|---|---|---|
| | male | female | male | female |
| 3週齢 | 12.08±0.76 | 11.65±1.32 | 9.98±1.12 | 9.5±0.68 |
| 12週齢 | 27.55±4.3 | 21.56±2.0 | 27.88±4.67 | 23.55±0.95 |

表２

| | | albumin | creatinin | BUN | total cholesterol |
|---|---|---|---|---|---|
| RG | male | 1.15± 0.24 | 0.28±0.08 | 78.83± 8.10 | 202.33± 32.71 |
| | female | 1.22± 0.26[b] | 0.35± 0.08[b] | 63.77± 12.23 | 125.33± 20.90[b] |
| GG | male | 1.58± 0.20 | 0.18± 0.04[a] | 44.08± 6.53[a] | 200.67± 60.50 |
| | female | 1.53± 0.14 | 0.13± 0.05[a] | 33.88± 6.83a | 125.83± 13.18[c] |

[a]: P<0.05 between between sex-matched gR
[b]: P<0.05 between male gR and female gR
[c]: P<0.05 between male gG and female gG

図２　Real time PCR の結果

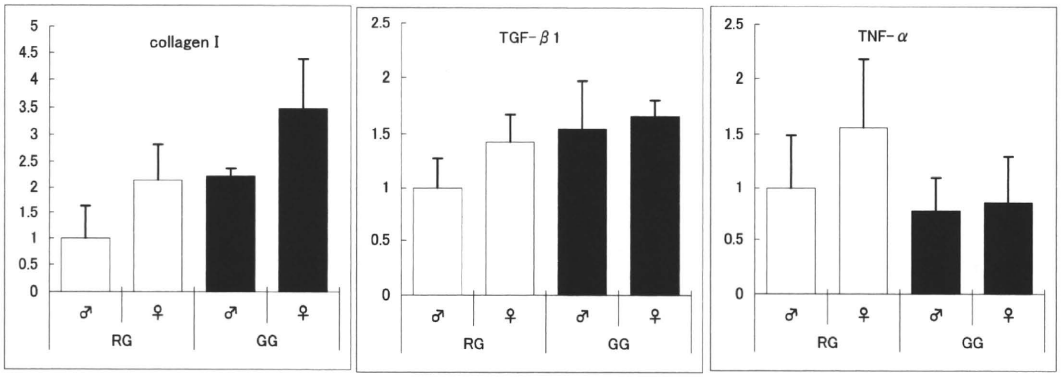


図３　PAS 染色の結果

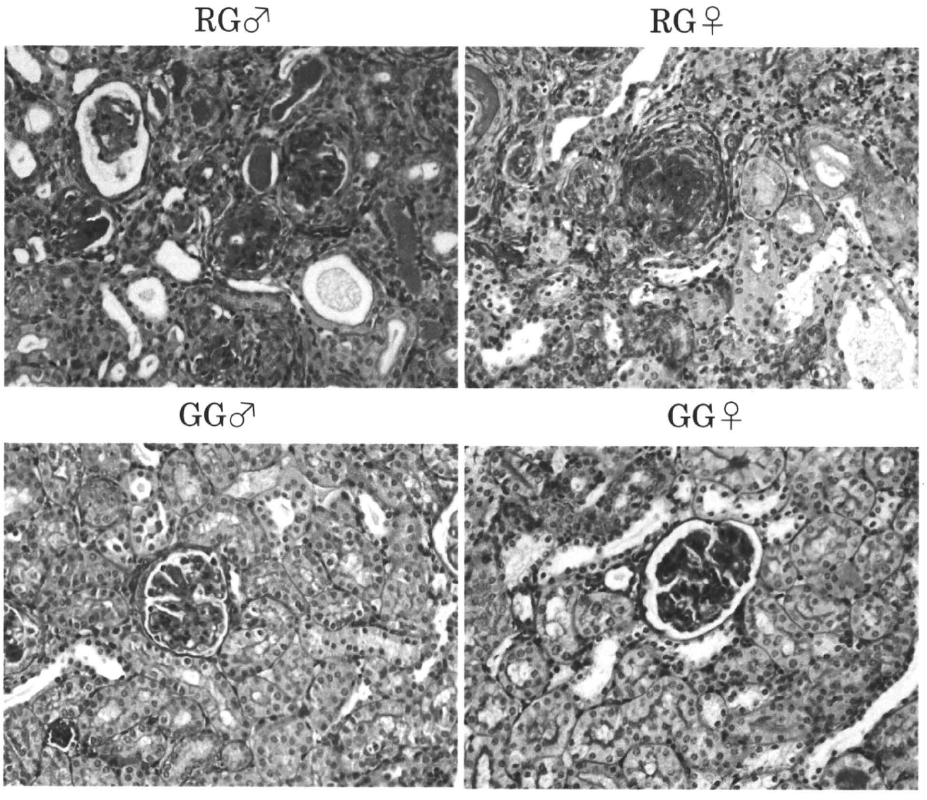

厚生労働科学研究費　(創薬基盤推進研究事業)
分担研究報告書

# 周産期疾患の解析と繁殖技術の開発のためのカニクイザル MHC class-I のタイピング解析とゲノムシーケンシング

分担研究者　高橋一朗　(医薬基盤研究所　難病・疾患資源研究部)
分担研究者　亀岡洋祐　(医薬基盤研究所　難病・疾患資源研究部)
研究協力者　東濃篤徳　(医薬基盤研究所　難病・疾患資源研究部)

## 研究要旨

周産期疾患の解析と繁殖技術の開発のためのカニクイザルのMHC class-Iのタイピング解析とゲノムシーケンシングの整備を目的として、MHC class-Iのタイピングの解析法の確立とアカゲザルをリファレンスとしたカニクイザルゲノムリシークエンスを行った。MHC class-Iのタイピングには Locus A はMAS Locus B は MBS のプライマーを用いた。カニクイザル家系における MHC class I Locus A および Locus B の発現を調べているが、現在そのうちの1頭につき MHC class I Locus A および Locus B のデータを示す。

カニクイザルゲノムリシークエンスに関してはCLC Genomics Workbenchによるアセンブリを行いアカゲザルゲノムの平均30倍以上の被覆率までシーケンスを行った。これらのコンティグでのSNP解析を行ったところ3M以上のSNPが見られその内0.3%程度が非同義置換であった。カニクイザルゲノム解析の使用に耐えうるためにIGV(Integrative genomics viewer)によるゲノム配列のブラウジングを可能にした。

これらの結果から周産期疾患の解析と繁殖技術の開発のためのカニクイザルゲノム解析に有用な研究ツールを整備・拡充できた。

## A. 研究目的

アカゲザルを中心としてマカクザルのMHC class-Iのタイピングおよびゲノム配列の整備が進められているが、カニクイザルに対するこれらの解析および情報の整備が遅れており、独立行政法人医薬基盤研究所が有するカニクイザルを用いた周産期疾患の解析と繁殖技術の開発のための遺伝子解析などに支障が生じていた。そこで我々はカニクイザルのMHC class-Iのタイピングとゲノムシーケンシングによる解析を試みた。

## B. 研究方法

1. DNA サンプルの調整:

医薬基盤研究所・霊長類医科学研究センターで飼育されているカニクイザル 7 頭から 10 ml の EDTA 加末梢血を得た。AllPrep DNA/RNA Mini Kit (QIAGEN)によって末梢血白血球からゲノミック DNA を調整した。

2. RNA サンプルの調整:

カニクイザル1家系5頭より全血を得、末梢血白血球を分離後 LPS 添加培地にて 1 晩培養し RNA を分離した。

3. cDNA の調整および増幅:

上記 RNA 試料を使い Random hexamer をプライマーとして 1 本鎖 cDNA を合成し、MHC class I タイピングプライマー MAS ( MHC type I Locus A ), MBS ( MHC type I Locus B ) ( Boyson et.al ) を用いPCR (変性94℃・アニーリング60℃・伸長72℃)反応を行った。増幅を確認後 PCR 産物を直接ベクターにクローニングし大腸菌を形質転換した。クローニングされたクローンをランダムに 10 数個分離し塩基配列をシーケンサー(ABI・ジェネティックアナライザ)で決定した。

4. カニクイザルゲノムリシークエンス:

医薬基盤研究所・霊長類医科学研究センターで飼育されている F1 世代のカニクイザルの末梢血 DNA をゲノムリシークエンスに用いた。ゲノムリシークエンスには SOLiD 3plus system(Life Tecnologies)を用いた。SOLiD 用のライブラリおよび DNA 断片付加ビーズは規定の方法で作製された。

5. カニクイザルゲノムリシークエンス解析:

ゲノムリシークエンスされたカニクイザルのゲノム配列をCLC Genomics Workbenchによってアカゲザルゲノムにマッピングし、SNP 解析を行った。

またカニクイザルゲノム配列を IGV(Integrative genomics viewer)でブラウジングできることによってカニクイザルゲノム解析に有用なツールの充実を目指した。

## C. 研究結果

1. MHC class-I のタイピング解析:

図 1 に解析したカニクイザル個体 A において発現している MHC class-I タイピング解析によって描かれたカニクイザル個体 A の系統樹を示す。図 1A は Locus A、図1B は Locus B について発現しているクローンの塩基配列の系統樹を示している。多個体の結果ではないので多くのことは言えないがすくなくとも 2 種類発現しておりヘテロであるといえる。

2. カニクイザルゲノムリシークエンス:

表 1 にカニクイザルのゲノム配列を CLC Genomics Workbench によってアカゲザルゲノムにマッピングした概略を示す。アカゲザルゲノムの平均 30 倍以上の被覆率までシーケンスを行うことができた。

3. SNP の検出と解析:

表2に今回検出した染色体毎のSNPおよび非同義置換の分布数(割合)を示す。アカゲザル染色体を基準として、3M 以上の SNP が見られその内 0.3%程度が非同義置換であることが明らかとなった。

4. カニクイザルゲノム配列の可視化

カニクイザルゲノム解析の効率化を目指し、カニクイザルゲノム配列を IGV(Integrative genomics viewer)でブラウジングできるように整備することができた(図 2)。

## D. 考察

カニクイザル MHC class-I のタイピング解析では Locus A および Locus B でいずれもアカゲザル MHC class I と近縁であることが明らかとなった。これらの解析によって描かれた系統樹からは maca-A-MAS-8, maca-A-MBS-8 がアカゲザル MHC class I の遠縁と考えられる。より正確な免疫遺伝情報を得るために今後さらに MHC class-I のタイピングの家系数を増やす必要があると思われる。

カニクイザルゲノムリシークエンスではアカゲザルゲノムの平均 30 倍以上の被覆率までシーケンスを行うことができたが、そのマッピング条件や SNP 検出条件を CLC Genomics Workbench の(ほぼ)初期値で行っているため精度の低い領域が存在する可能性がある。今後はコンティグの精度を向上させるためにマッピングおよび SNP 検出の条件検討を行うとともに他の解析ツール(Bioscope など)を併用することによってデータセットの信頼度を高める必要がある。

今後は得られたカニクイザル MHC class-I のタイピング結果およびカニクイザルゲノムデータセットを用いて IGV(Integrative genomics viewer)などを応用してデータベース化することで周産期疾患の解析と繁殖技術の開発のための遺伝解析やゲノム解析に貢献することができると考えられた。

## E. 結論

今回解析しつつある MHC class-I のタイピング結果から家系による免疫情報の遺伝解析が可能となることが予想できる。 MHC に先駆けて進んでいるカニクイザルゲノムデータではアカゲザルゲノムの平均 30 倍以上の被覆率までシーケンスを行うことができ、SNP 解析から 3M 以上の SNP が見られその内 0.3%程度が非同義置換であることが明らかとなった。

今後 MHC class-I LucusA, Locus B のタイピングの家系数を増やし免疫情報の遺伝解析およびゲノムデータセットの解析を続けていく必要性が考えられた。

## F. 研究発表

1. 学会発表

(1)東濃篤徳、長田直樹、亀岡洋祐、高橋一朗、保富康弘、寺尾恵治, TOOLS FOR GENETIC ANALYSIS OF CYNOMOLGUS MACAQUES, 国際霊長類学会, 2010 年 9 月 13 日

(2) 東濃篤徳、長田直樹、坂手龍一、平田誠、亀岡洋祐、保富康弘、高橋一朗, 次世代シークエンサーを用いたカニクイザルにおける遺伝子発現解析, 分子生物学会, 2010 年 12 月 7 日

## G. 知的財産権の出願・登録状況

なし

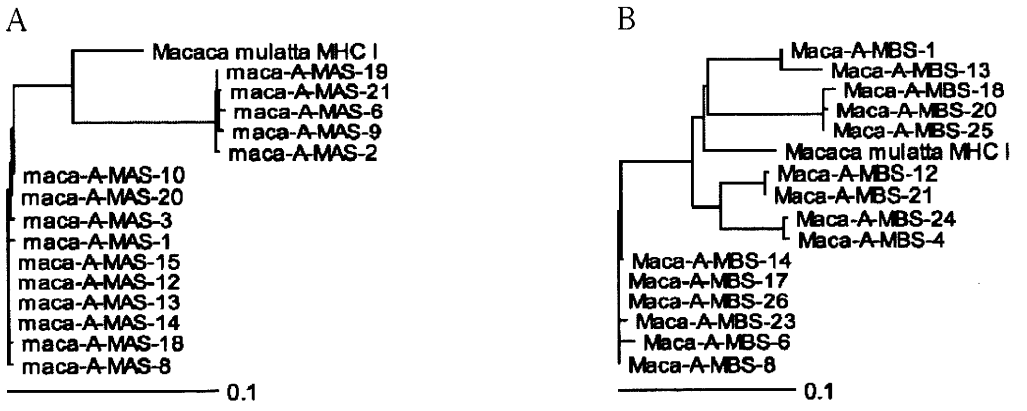


図１．個体Ａ　における MHC type Ⅰ 発現クローンの系統樹
A. Locus A の発現クローン　B. Locus B の発現クローン

| ゲノムマッピング概略 | |
|---|---|
| アカゲザルゲノム総塩基長（bp） | 2,863,681,749 |
| カニクイザルゲノム解読総リード数（tags） | 2,392,801,894 |
| カニクイザルゲノム解読総塩基数（bp） | 88,733,138,026 |
| カニクイザルゲノム解読総塩基長（bp） | 2,640,359,382 |
| カニクイザルゲノム解読総塩基長のアカゲザルゲノム総塩基長に対する割合（％） | 92.0 |
| カニクイザルゲノム解読総塩基のアカゲザルゲノム総塩基に対する平均被覆回数（回） | 30.7 |

表 1．CLC Genomics Workbench によるカニクイザルゲノムマッピング概略

| | SNP数 | 非同義置換SNP数 | 率 (%) |
|---|---|---|---|
| 染色体1 | 311,927 | 1283 | 0.41 |
| 染色体2 | 260,944 | 687 | 0.26 |
| 染色体3 | 253,171 | 708 | 0.28 |
| 染色体4 | 233,282 | 671 | 0.29 |
| 染色体5 | 251,993 | 450 | 0.18 |
| 染色体6 | 247,055 | 585 | 0.24 |
| 染色体7 | 234,443 | 844 | 0.36 |
| 染色体8 | 201,263 | 416 | 0.21 |
| 染色体9 | 185,530 | 490 | 0.26 |
| 染色体10 | 134,878 | 508 | 0.38 |
| 染色体11 | 181,741 | 687 | 0.38 |
| 染色体12 | 141,656 | 396 | 0.28 |
| 染色体13 | 189,177 | 460 | 0.24 |
| 染色体14 | 180,056 | 768 | 0.43 |
| 染色体15 | 155,955 | 438 | 0.28 |
| 染色体16 | 104,226 | 656 | 0.63 |
| 染色体17 | 139,365 | 303 | 0.22 |
| 染色体18 | 107,882 | 206 | 0.19 |
| 染色体19 | 64,929 | 897 | 1.38 |
| 染色体20 | 116,344 | 548 | 0.47 |
| 染色体X | 147,207 | 341 | 0.23 |
| 染色体m | 39 | 9 | 23.08 |

表 2. 検出した染色体毎の SNP および非同義置換の分布数(割合)

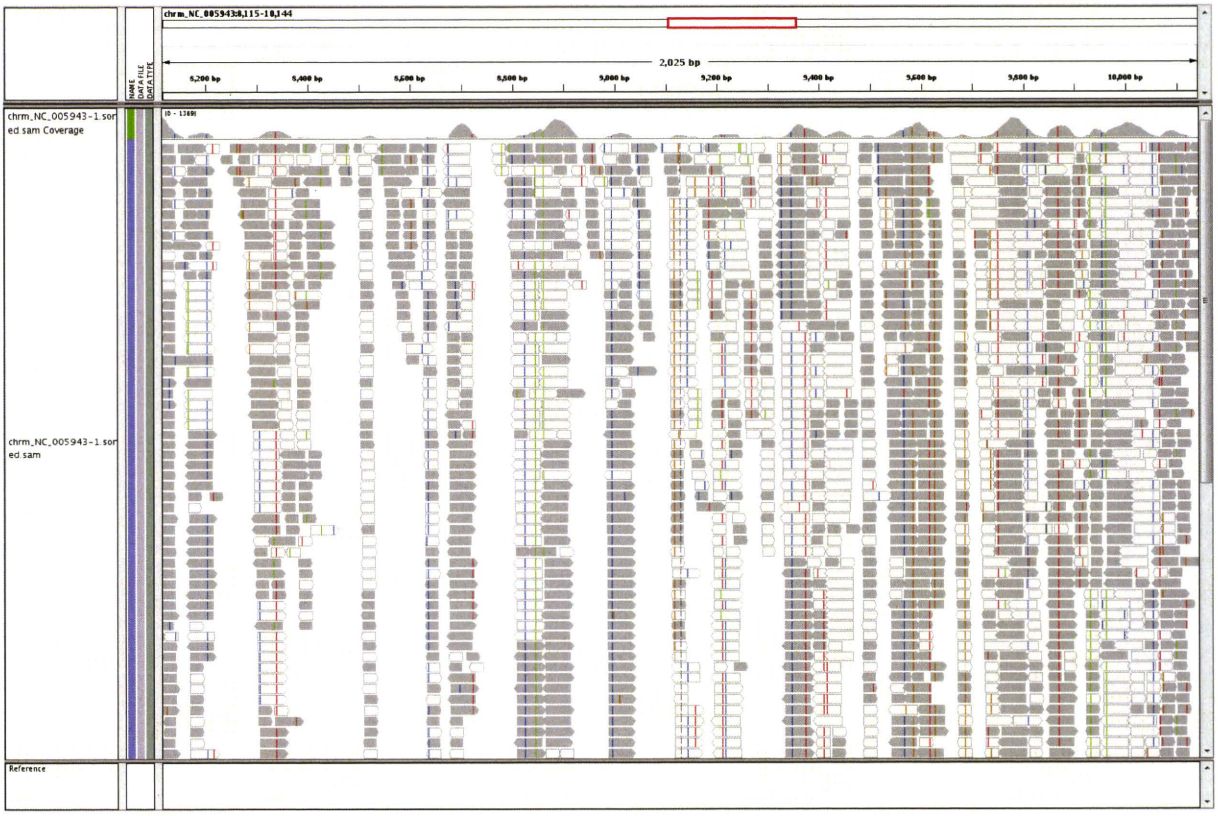


図 2. IGV(Integrative genomics viewer)によるカニクイザルゲノム配列の可視化(ミトコンドリア染色体)

# 研究成果の刊行に関する一覧表

（平成２２年度）

研究成果の刊行に関する一覧表

書籍

| 著者氏名 | 論文タイトル名 | 書籍全体の編集者名 | 書　籍　名 | 出版社名 | 出版地 | 出版年 | ページ |
|---|---|---|---|---|---|---|---|
| 山田-内尾こずえ・眞鍋昇 | 腎疾患 自然発症モデル 「ネフローゼ症候群モデル（ICGNマウス）」 | 北徹・堀内久徳・柳田素子・猪原匡史・冨本秀和・並河徹 | 循環器疾患-疾患モデルの作製と利用 | 株式会社エル・アイ・シー | 東京 | 2010 | 260-263 |

雑誌

| 発表者氏名 | 論文タイトル名 | 発表誌名 | 巻号 | ページ | 出版年 |
|---|---|---|---|---|---|
| .Yoshida,T., Saito,A., Iwasaki,Y.,Iijima,S., Kurosawa,T., Katakai,Y., Yasutomi,Y.,Reimann,K.A., Hayakawa,T. and Akari,H. | Characterization of natural killer cells in tamarins: a technical basis for studies of innate immunity. | Frontiers Microbiol. | 印刷中 | | 2011 |
| Xing, Li., Wang, J.C., Li, T-C., Yasutomi,Y., Lara,J., Khurdyakaov,Y., Schofield D., Emerson,S., Purcell,R., Takeda,N., Miyamura,T. and Holland,R.C. | Spatial configuration of hepatitis E virus antigenic domain. | J.Virol. | 85 | 1117-1124 | 2011 |

| 発表者氏名 | 論文タイトル名 | 発表誌名 | 巻号 | ページ | 出版年 |
|---|---|---|---|---|---|
| Chono,H., Matsumoto,K., Tsuda,H., Saito,N., Lee,K.., Kim,S., Shibata,H., Ageyama,N., Terao,K., Yasutomi,Y., Mineno J., Kim,S., Inoue,M. and Kato,I. | Acquistion of HIV-1 resistance in T lymphocytes using an ACA-specific E.coli mRNA interferase. | Human Gene Ther. | 22 | 35-43 | 2011 |
| Saito,A., Nomaguchi,M., Iijima,S.,Lee,Y-J., Kono,K., Nakayama,E.E., Shioda,T., Yasutomi,Y., Adachi,A., Matano,T., Akari,H. | A novel monkey-tropic HIV-1 derivative encoding only minimal SIV sequences can replicate in cynomolgus monkeys. | Micorbes Infect | 13 | 58-64 | 2011 |
| Naruse,T.K., Zhiyong,C., Yanagida,R., Yamashita,T., Saito,Y., Mori,K., Akari,H., Yasutomi,Y., Matano,T. and Kimura,A. | Diversity of MHC class I genes in Burmese-origine rhesus macaques. | Immunogenetics | 62 | 601-611 | 2010 |
| Okabayashi,S., Uchida,K., Nakayama,H., Ohno,C., Hanari,K., Goto,I. and Yasutomi,Y. | Periventricular Leucomalacia (PVL)-like lesions in two neonatal cynomolgus monkeys (macaca fascicularis) | J.Comp.Pathol. | Epub | | 2010 |

| 発表者氏名 | 論文タイトル名 | 発表誌名 | 巻号 | ページ | 出版年 |
|---|---|---|---|---|---|
| Yasuhiro Yasutomi. | Establishment of Specific Pathogen-Free Macaque Colonies in Tsukuba Primate Research Center of Japan for AIDS research. | Vaccine | B | 75-77. | 2010 |
| Fujimoto,K., Takano,J., Narita,T., Hanari,K., Shimozawa,N., Sankai,T., Yoshida T., Terao,K., Kurata,T. and Yasutomi,Y. | Simian Retrovirus type D infection in a colony of cynomolgus monkeys. | Comp.Med. | 60 | 51-53. | 2010 |
| Cueno,M.E., Karamatsu,K., Yasutomi, Y., Laurena,A.C. and Okamoto.T. | Preferential expression and immunogenicity of HIV-1 Tat fusion protein expressed in tomato plant. | Transgenic Res. | 19 | 889-895 | 2010 |
| J. Yamasaki, C. Iwatani, H. Tsuchiya, J. Okahara, T. Sankai, R. Torii | Vitrification and transfer of cynomolgus monkey (*Macaca fascicularis*) embryos fertilized by intracytoplasmic sperm injection | Theriogenology | in press | | |
| T. Sankai, N. Owada, K. Kyono | Cryopreservation of the ovary (Review) | J. Mamm. Ova Res. | 27 | 101-105 | 2010 |
| T. Yoshida, K. Hanari, K. Fujimoto, T. Sankai | Female reproduction characteristics in a large-scale breeding colony of cynomolgus monkeys (*Macaca fascicularis*) | Exp. Anim. | 59 | 251-254 | 2010 |
| N. Shimozawa, S. Nakamura, I. Takahashi, M. Hatori, T. Sankai | Characterization of a novel embryonic stem cell line in the African green monkey (Cercopithecus aethiops) | Reproduction | 139 | 565-573 | 2010 |

| 発表者氏名 | 論文タイトル名 | 発表誌名 | 巻号 | ページ | 出版年 |
|---|---|---|---|---|---|
| K. Fujiomto, J. Takano, T. Narita, K. Hanari, N. Shimozawa, T. Sankai, T. Yosida, K. Terao, T. Kurata, Y. Yasutomi | Simian Retrovirus Type D Infection in a Colony of Cynomolgus Monkeys | Comp. Med. | 60 | 51-53 | 2010 |
| Yuki Y, Nochi T,Harada N, KatakaiY, Shibata H, Mejima M, Kohda T, Tokuhara D, Kurokawa S, TakahashiY, Ono F, KozakiS, Terao K, Tsukada H, Kiyono H. | In vivo molecular imaging analysis of a nasal vaccine that induces protective immunity against botulism in nonhuman primates. | Journal of Immunology. | 185 | 5436-5443 | 2010 |
| Chono H, Matsumoto K, Tsuda H, Saito N, Lee K, Kim S, Shibata H,Ageyama N, TeraoK, Yasutomi Y, Mineno J, Kim S, Inouye M, Kato I. | Acquisition of HIV-1 resistance in T lymphocytes using an ACA-specific *E. coli* mRNA interferase. | Human Gene Therapy. | 22 | 35-43 | 2011 |
| Yoshino N, Kanekiyo M, Hagiwara Y, Okamura T, Someya K, Matsuo K, Ami Y, Sato S, Yamamoto N, Honda M. | Intradermal delivery of recombinant vaccinia virus vector DIs induces gut-mucosal immunity. | Scand. J. Immunol. | 72(2) | 98-105 | 2010 |

| 発表者氏名 | 論文タイトル名 | 発表誌名 | 巻号 | ページ | 出版年 |
|---|---|---|---|---|---|
| Shiozuka C, Taguchi A, Matsuda J, Noguchi Y, Kunieda T, Uchio-Yamada K, Yoshioka H, Hamanaka R, Yano S, Yokoyama S, Mannen K, Kulkarni AB, Furukawa K, Ishii S. | Increased globotriaosylceramide levels in a transgenic mouse expressing human {alpha}1,4-galactosyltransferase and a mouse model for treating Fabry disease. | J Biochem. | 149(2) | 161-170 | 2011 |
| Takeda S, Sato N, Uchio-Yamada K, Sawada K, Kunieda T, Takeuchi D, Kurinami H, Shinohara M, Rakugi H, Morishita R. | Diabetes-accelerated memory dysfunction via cerebrovascular inflammation and Abeta deposition in an Alzheimer mouse model with diabetes. | Proc Natl Acad Sci U S A. | 107(15) . | 7036-7041 . | 2010 |

frontiers in
MICROBIOLOGY

ORIGINAL RESEARCH ARTICLE
published: xx November 2010
doi: 10.3389/fmicb.2010.00128

# Characterization of natural killer cells in tamarins: a technical basis for studies of innate immunity

**Tomoyuki Yoshida[1,2†], Akatsuki Saito[2,3†], Yuki Iwasaki[1,4], Sayuki Iijima[1], Terue Kurosawa[1], Yuko Katakai[5], Yasuhiro Yasutomi[6], Keith A. Reimann[7], Toshiyuki Hayakawa[2] and Hirofumi Akari[1,2]***

[1] *Tsukuba Primate Research Center, National Institute of Biomedical Innovation, Tsukuba, Ibaraki, Japan*
[2] *Primate Research Institute, Kyoto University, Inuyama, Aichi, Japan*
[3] *International Research Center for Infectious Diseases, The Institute of Medical Science, The University of Tokyo, Minato-ku, Tokyo, Japan*
[4] *Graduate School of Medicine and Dentistry, Tokyo Medical and Dental University, Bunkyo-ku, Tokyo, Japan*
[5] *Corporation for Production and Research of Laboratory Primates, Tsukuba, Ibaraki, Japan*
[6] *Laboratory of Immunoregulation and Vaccine Research, Tsukuba Primate Research Center, National Institute of Biomedical Innovation, Tsukuba, Ibaraki, Japan*
[7] *Division of Viral Pathogenesis, Beth Israel Deaconess Medical Center, Harvard Medical School, Boston, MA, USA*

***Edited by:***
*Yasuko Yokota, National Institute of Infectious Diseases, Japan*

***Reviewed by:***
*Koji Ishii, National Institute of Infectious Diseases, Japan*
*Ikuo Shoji, Kobe University Graduate School of Medicine, Japan*

***Correspondence:**
*Hirofumi Akari, Primate Research Institute, Kyoto University, Inuyama, Aichi 484-8506, Japan.*
*e-mail: akari@pri.kyoto-u.ac.jp*

†*Tomoyuki Yoshida and Akatsuki Saito have contributed equally to this work.*

Natural killer (NK) cells are capable of regulating viral infection without major histocompatibility complex restriction. Hepatitis C is caused by chronic infection with hepatitis C virus (HCV), and impaired activity of NK cells may contribute to the control of the disease progression, although the involvement of NK cells *in vivo* remains to be proven. GB virus B (GBV-B), which is genetically most closely related to HCV, induces acute and chronic hepatitis upon experimental infection of tamarins. This non-human primate model seems likely to be useful for unveiling the roles of NK cells *in vivo*. Here we characterized the biological phenotypes of NK cells in tamarins and found that depletion of the CD16$^+$ subset *in vivo* by administration of a monoclonal antibody significantly reduced the number and activity of NK cells.

**Keywords: CD16, cynomolgus monkey, tamarin, NK cell**

## INTRODUCTION

Natural killer (NK) cells are a component of the innate immune system that play a central role in host defense against viral infection and tumor cells. Much of the evidence for a role for NK cells in controlling viral infections has come from experiments with mice that were genetically modified (Lian and Kumar, 2002) or were treated with NK cell-depleting antibodies (Kasai et al., 1980) or from the study of humans with inherited NK cell deficiencies (Biron et al., 1989; Orange, 2002).

NK cells can be rapidly recruited into infected organs and tissue by chemoattractant factors produced by virus-infected cells and activated resident macrophages, which are also a major source of interferon (IFN), which induces NK cell proliferation, NK cell-mediated cytolysis of virus-infected cells, and the secretion of chemokines (Robertson, 2002). NK cells can kill virus-infected cells by using cytotoxic granules or by recognizing and inducing lysis of antibody-coated target cells (antibody-dependent cell cytotoxicity) via antibody binding receptor CD16. For instance, human blood NK cells are cytotoxic against dengue virus-infected cells in target organs via direct cytolysis and antibody-dependent cell-mediated cytotoxicity (reviewed by Navarro-Sánches et al., 2005). Early activity of NK cells may be important for clearing acute infections such as that of dengue virus. However, the effect that NK cells may exert on chronic infections with viruses such as hepatitis C virus (HCV) is less clear.

HCV is the causative agent of chronic hepatitis C, cirrhosis, and finally liver cancer. In general, acquired and innate immunity induced by acute HCV infection is not sufficient for the viral clearance, and persistent HCV infection frequently leads to progression to chronic hepatitis (reviewed by Cheent and Khakoo, 2010). It was reported that dendritic cells (DCs) in HCV infection were not responsive to IFN-α, and thus failed to promote subsequent activation of NK cells as a primary innate immune response (reviewed by Kanto, 2008). This is in agreement with the finding that the killing activity of NK cells in patients with chronic hepatitis C is inactivated in *in vitro* studies (Deignan et al., 2002; Golden-Mason et al., 2008). These data suggest that the dysfunction of NK cells contributes to the persistent infection of HCV and chronic hepatitis. On the other hand, it was suggested that inappropriately activated NK cells caused liver injury after the viral infection (Liu et al., 2000). The population of NK cells is relatively minor in peripheral lymphoid organs but is abundant in liver, raising a question as to their function in the innate immune response to acute and chronic HCV infection in the liver. It is possible that NK cells partially regulate the replication of HCV in this organ during early infection whereas they promote the liver dysfunction in chronic HCV infection. To examine these possibilities, it is necessary to clarify the involvement of NK cells *in vivo* in HCV infection. However, it is questionable whether the results of *ex vivo* analyses of NK cells would reflect their actual roles *in vivo*. Therefore, it might be more informative to study the function of NK cells directly by means of *in vivo* depletion technique in animal models.

A chimpanzee model of HCV infection has frequently been employed to evaluate the role of acquired antiviral immune responses, although the involvement of NK cells has not been fully evaluated because of the limitations on the use of chimpanzees

due to ethical and financial restrictions (Cohen and Lester, 2007). Accordingly, New World monkeys infected with GB virus B (GBV-B) appear to be a promising model because (i) among viruses so far known, GBV-B is genetically the most closely related to HCV and can infect New World monkeys, including tamarins, marmosets and owl monkeys, but not Old World monkeys (reviewed by Akari et al., 2009), (ii) tamarins develop acute and chronic hepatitis after experimental GBV-B infection (Bukh et al., 1999; Sbardellati et al., 2001; Lanford et al., 2003; Martin et al., 2003; Ishii et al., 2007; Takikawa et al., 2010), (iii) the infection induces antiviral cellular immune responses (Woollard et al., 2008), and (iv) tamarins and marmosets are commercially available and easily handled, reared and bred. Moreover, tamarins, being primates, may have a similar immune system to humans, and therefore they may be useful for studying the function of NK cells against the hepatitis virus in this tamarin model.

Our final goal is to study the role of NK cells as a major player in innate immunity during the course of the progression of viral hepatitis. Since some basic information regarding the biological characteristics of NK cells still remains unclear, we initially sought to characterize NK cells in tamarins to provide a technical basis for further studies.

## MATERIALS AND METHODS

### ANIMALS

Five red-handed tamarins (*Saguinus midas*) and five cynomolgus monkeys (*Macaca fascicularis*) were used in this study. The animals were cared for in accordance with National Institute of Biomedical Innovation rules and guidelines for experimental animal welfare, and all protocols were approved by our Institutional Animal Study Committee.

### FLOW CYTOMETRY

Flow cytometry was performed as previously described (Akari et al., 1997) with a slight modification. Fifty microliters of whole blood from cynomolgus monkeys and tamarins was stained with combinations of fluorescence-conjugated monoclonal antibodies (mAb): anti-CD3 (SP34-2; Becton Dickinson), anti-CD4 (L200; BD Pharmingen), anti-CD8 (CLB-T8/4H8; Sanquin), anti-CD16 (3G8; BD Pharmingen), and anti-CD16 (DJ130c; Dako). Then, erythrocytes were lysed with FACS lysing solution (Becton Dickinson). After having been washed with sample buffer containing phosphate-buffered saline (PBS), 1% fetal calf serum (FCS), and 1% formaldehyde, the labeled cells were resuspended in the sample buffer. The expression of the immunolabeled molecules on the lymphocytes was analyzed with a FACSCanto II flow cytometer (Becton Dickinson). Peripheral blood mononuclear cells (PBMCs) were separated from the blood of these monkeys by a Ficoll-Paque gradient method. The cells were resuspended in complete medium composed of RPMI-1640 medium supplemented with 10% FCS, 1% penicillin/streptomycin, 2 mM HEPES and 55 μM 2-mercaptoethanol at 4°C until use. Fluorochrome-labeled mouse mAbs were reacted with $2 \times 10^5$ PBMCs at 4°C for 30 min. The labeled cells were washed with PBS containing 1% FCS, and resuspended in the sample buffer. The expression of the immunolabeled molecules on the lymphocytes was analyzed as mentioned above.

### FLOW CYTOMETRIC 5-(AND 6)-CARBOXYFLUORESCEIN DIACETATE SUCCINIMIDYL ESTER (CFSE)/7-AMINO ACTINOMYCIN D (7-AAD) CYTOTOXIC ASSAY

Peripheral blood mononuclear cells were separated from the blood of these monkeys by a Ficoll-Paque gradient method. These PBMCs were then resuspended in complete medium at 37°C until use. The flow cytometric CFSE/7-AAD cytotoxicity assay was performed as previously described (Lecoeur et al., 2001) with slight modifications. K562 cells ($3 \times 10^6$) were labeled with 500 nM CFSE (from a 1 mM stock solution in dimethyl sulfoxide [Sigma] stored at −20°C) in Hanks' Balanced Salt Solution for 8 min at 37°C in total of 2 ml. The cells were then washed twice in complete medium and used immediately for the cytotoxicity assay. The CFSE-labeled target cells (20,000 cells) were used at different E (effector):T (target) ratios (0:1, 3:1, and 9:1). After 24 h incubation, the cells were stained with 0.25 μg/ml of 7-AAD and incubated for 10 min at 37°C in a $CO_2$ incubator. The cells were washed twice with 1% FCS–PBS, resuspended in sample buffer and analyzed immediately by flow cytometry.

### MAGNETIC CELL SEPARATION

Magnetic cell separation (MACS) was performed as previously described (Tenorio and Saavedra, 2005) with slight modifications. PBMCs ($1 \times 10^7$) were washed with 3 ml of MACS buffer composed of PBS with 2 mM EDTA and 0.5% bovine serum albumin, and resuspended in 100 μl of the same buffer. Ten microliters of fluorescein isothiocyanate (FITC)-labeled anti-CD16 mAb (3G8) was added. The cells with or without the mAb were incubated for 10 min at 4°C, washed with 1 ml of MACS buffer, and resuspended in 80 μl of the same buffer. They were mixed with 20 μl of anti-FITC MicroBeads and incubated for 15 min at 4°C, washed with 1 ml of MACS buffer, and resuspended in 500 μl of the same buffer. The CD16-positive cells were separated by negative selection using LD columns and a MACS separation unit following the instructions provided by the manufacturer (Miltenyi Biotec). CD16-negative cells were resuspended in complete medium and co-cultured with K562 cells at 37°C for the NK cytotoxicity assay immediately.

### DETECTION OF CIRCULATING ANTI-CD16 MAB (3G8)

Concentrations of an anti-CD16 antibody (3G8) in plasma samples were assessed using a mouse $IgG_1$ Quantitative ELISA Kit (Bethye Laboratory, Inc.). The assay was performed according to the manufacturer's instruction with a slight modification. To detect the mAb in monkey plasma, 96-well enzyme-linked immunosorbent assay (ELISA) plates were coated with a capture antibody and incubated for 1 h at 37°C and washed with wash solution (50 mM Tris, 0.14 M NaCl, 0.05% Tween 20, pH 8.0) three times. The plates were blocked with blocking solution (Postcoat) for 30 min at 37°C. Plasma samples from antibody-treated monkeys were diluted in dilution buffer (50 mM Tris, 0.14 M NaCl, 1% bovine serum albumin, 0.05% Tween 20, pH 8.0), applied to the wells in serial dilutions, incubated for 1 h at 37°C and washed with the wash solution five times. Goat anti-mouse $IgG_1$ conjugated with horseradish peroxidase and diluted 1:50000 in dilution buffer was added to each well and incubated for 1 h at 37°C. Each well was washed with the wash solution five times. Substrate solution was added to each well and incubated

for 10–15 min at room temperature, and then the reaction was stopped with $H_2SO_4$. Optical density was measured using an ELISA reader at 450 nm.

### *IN VIVO* DEPLETION OF CD16 POSITIVE CELLS

Mouse anti-human CD16 (3G8) mAb (Fleit et al., 1982) was produced in serum-free medium and purified using protein A affinity chromatography. Endotoxin levels were lower than 1 EU/mg. The antibody was administered to tamarins (Tm 05-003, Tm 06-020) and cynomolgus monkeys (Mf 00-005, Mf 99-110) intravenously at 50 mg/kg at a rate of 18 ml/min using a syringe pump. Lymphocyte subsets were monitored for 3 weeks after the administration.

### STATISTICAL ANALYSIS

Statistical analyses of lymphocyte ratios were performed using Student's *t*-test and single-factor ANOVA, followed by Fisher's protected least-significant difference *post hoc* test by using StatView software (SAS Institute, NC, USA). The results were confirmed in more than three independent experiments in tamarins and cynomolgus monkeys.

## RESULTS

### LYMPHOCYTE SUBSETS IN TAMARINS

First, we examined the lymphocyte subsets in tamarins as compared with cynomolgus monkeys (**Figure 1**). The percentages of T and B lymphocytes indicated as $CD20^-CD3^+$ and $CD20^+CD3^-$ subsets in the total lymphocytes were found to be 68.8% (range 41.9–68.8%) and 12.3% (range 11.8–12.6%) in tamarins and 68.4% (range 42.6–68.4%) and 10.2% (range 9.1–11.4%) in cynomolgus monkeys, respectively. The percentage of $CD4^+$ T cells in the $CD3^+$ subset was 45.5% (range 41.9–52.5%) and 55.3% (range 42.6–64.4%) while that of $CD8^+$ T cells was 41.0% (range 35.8–44.5%) and 31.2% (range 29.3–34.6%) in tamarins and cynomolgus monkeys, respectively. Next, the NK cell subset was determined as $CD3^-$ $CD16^+$ lymphocytes in this study. The percentage of NK cells was 30.5% (range 16.9–52.5%) and 18.9% (range 13.7–22.4%) in tamarins and cynomolgus monkeys, respectively. We analyzed statistically whether these lymphocyte ratios were different between tamarins and cynomolgus monkeys, and found that there were no significant differences of the lymphocyte ratios between them. We therefore concluded that the proportions of the major lymphocyte subsets in tamarins were relatively similar to those in cynomolgus monkeys.

### FLUORESCENCE-BASED *IN VITRO* ASSAY FOR QUANTITATIVELY EVALUATING NATURAL KILLER ACTIVITY

Natural killer cell cytotoxic assays conventionally require considerable numbers of PBMCs, and this has been a major hurdle for analyzing the NK activity in small New World monkeys due to the limited availability of their blood. Therefore, we employed an alternative method using a fluorescence-based assay to assess the activity of NK cells in tamarins as previously described (Lecoeur et al., 2001) with slight modifications. When CFSE-stained K562 target cells were incubated with the effector PBMCs obtained from tamarins at an effector/target (E/T) ratio of 9:1, 42% of the K562 cells were positive for 7-AAD, which stains apoptotic cells (**Figure 2A**). We

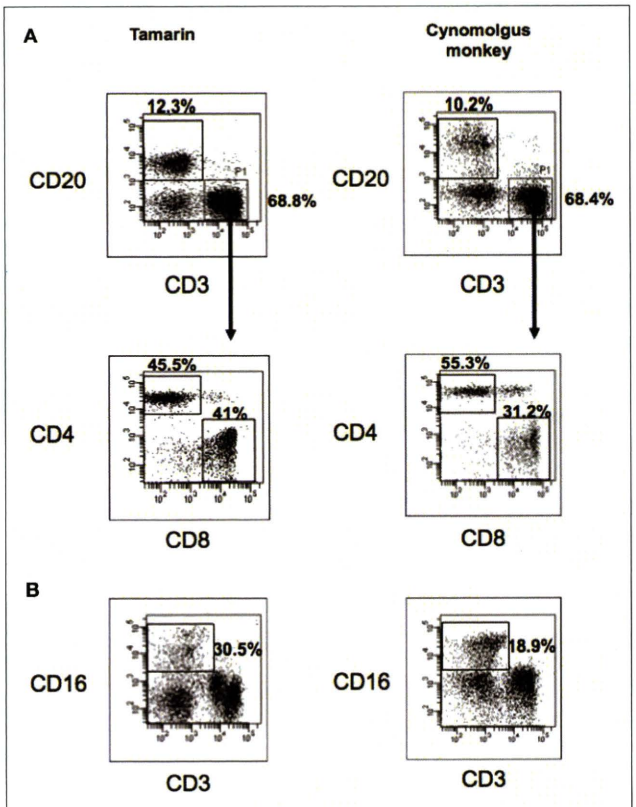


**FIGURE 1 | Flow cytometric analysis of CD3, CD20, CD4, CD8, and CD16 expression on lymphocytes in cynomolgus monkeys and tamarins.** Representative results in tamarins and cynomolgus monkeys are shown. **(A)** Flow cytometric analysis of CD3 and CD20 expression in lymphocytes (top panels) and CD4 and CD8 expression in $CD3^+$ population (bottom panels) of both monkeys. **(B)** Flow cytometric analysis of CD3 and CD16 expression in both monkey species. The numbers denote the percentages of lymphocytes. We analyzed statistically whether these lymphocyte ratios were different between tamarins and cynomolgus monkeys by using StatView software. There were no significant differences of the lymphocyte ratios between them.

confirmed that the killing activity of NK cells was dose-dependent, and that the level in tamarins was higher than that in cynomolgus monkeys (**Figures 2B and 3**).

Next, in order to examine if $CD16^+$ lymphocytes represent a major population with NK activity, $CD16^-$ PBMCs were obtained by negative selection using MACS (**Figure 4A**) in both tamarins and cynomolgus monkeys. We found that depletion of $CD16^+$ cells greatly attenuated the killing activity in both tamarins and cynomolgus monkeys (**Figure 4B**), indicating that $CD16^+$ lymphocytes are a major population with NK activity.

### *IN VIVO* DEPLETION OF $CD16^+$ NK CELLS USING A MURINE ANTI-CD16 MAB

We next sought to establish a system to directly evaluate the role of NK cells in tamarins. We asked if the administration of an anti-CD16 (3G8) mAb could deplete $CD16^+$ lymphocytes *in vivo*. Tamarins were intravenously administered 3G8 or control mAb (MOPC-21) at a dose of 50 mg/kg. Using an anti-CD16 antibody that is not cross-blocked by 3G8 (clone DJ130c), it was found that at

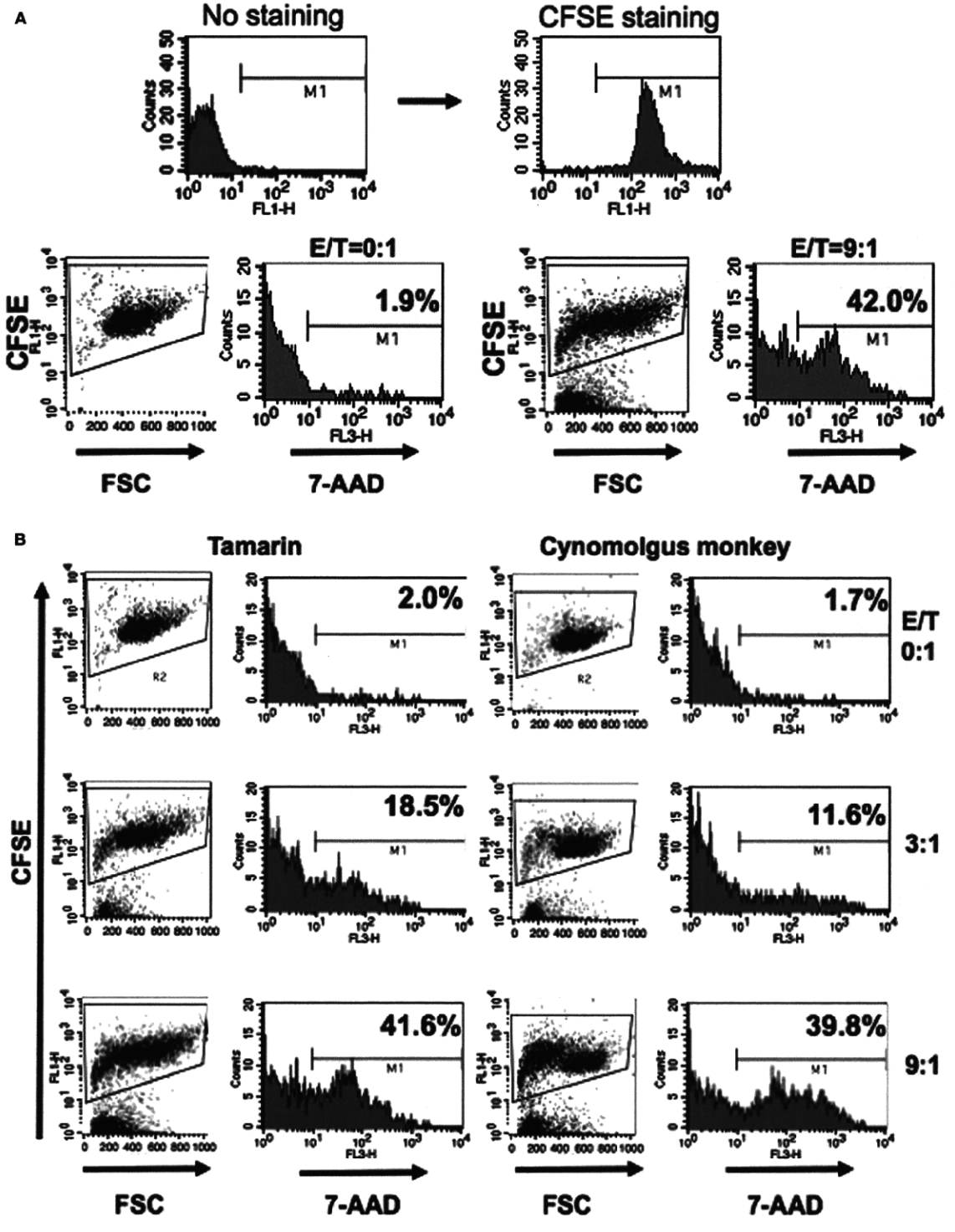


**FIGURE 2 | Cytotoxicity assay by CFSE and 7-AAD staining. (A)** CFSE-stained K562 cells were co-cultured with PBMCs at E/T ratios of 9:1 and 0:1. The CFSE-stained K562 cells were first gated by FSC and SSC characteristics, and 3000 events were captured. **(B)** CFSE-stained K562 target cells were killed by tamarin PBMCs using E/T ratios of 9:1, 3:1, and 0:1. The numbers in the panels denoted the percentages of 7-AAD positive cells. We analyzed statistically whether these killing activities were different between tamarins and cynomolgus monkeys by using StatView software.

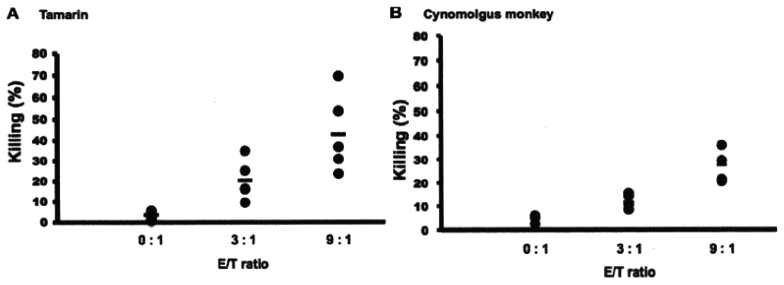


**FIGURE 3 | Dose-dependency of killing activity of NK cells in tamarins. (A,B)** K562 target cells were stained with CFSE and co-cultured with PBMCs as described in Section "Materials and Methods". CFSE-stained K562 target cells were killed by PBMCs of tamarins and cynomolgus monkeys in a dose-dependent manner. For all experiments, the number of observations used to calculate the mean were $n = 5$. We analyzed statistically whether these killing activities were different between tamarins and cynomolgus monkeys by using StatView software.

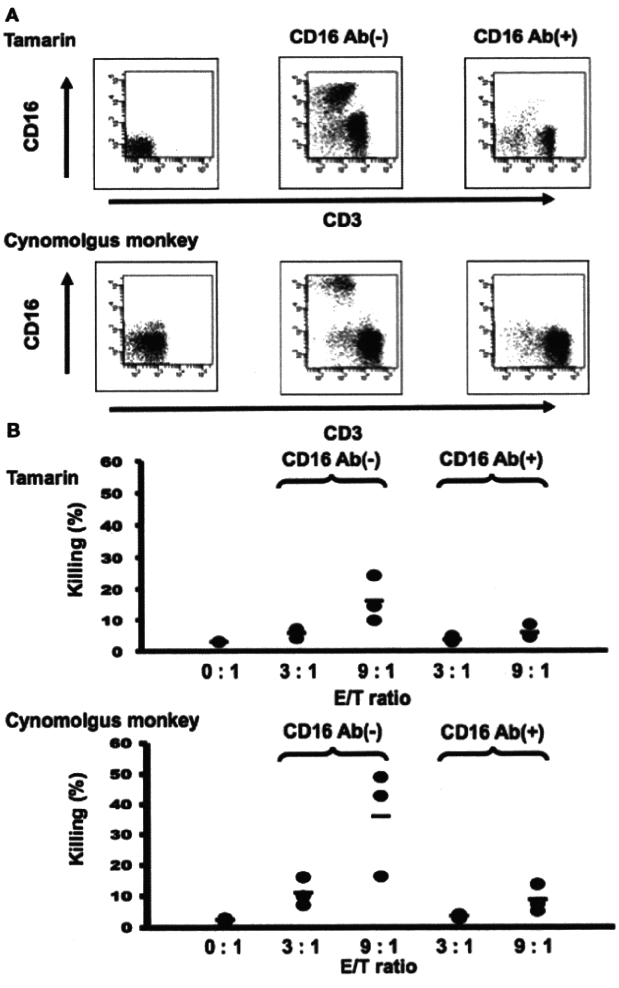


**FIGURE 4 | CD16⁺ cells were a major population with natural killer activity in tamarins. (A)** CD16⁺ cells were depleted from PBMCs by MACS as described in Section "Materials and Methods". CD16⁻ PBMCs were obtained by negative selection using MACS. **(B)** K562 cells were stained with CFSE and co-cultured with CD16-treated or untreated PBMCs as described in Section "Materials and Methods". Results shown are representative of three independent experiments.

1–3 days after the treatment CD16$^+$ cells were completely depleted, followed by recovery to the initial levels at around 2 weeks after the administration, which was consistent with the results in cynomolgus monkeys (**Figure 5B**). It is noteworthy that the numbers of CD4$^+$/CD8$^+$ T and B lymphocytes were not affected by the treatment and that administration of control antibody did not deplete CD16$^+$ cells during the period tested (data not shown), showing that the effect of 3G8 on CD16$^+$ cells was specific (data not shown). We also measured the concentration of the 3G8 mAb in the plasma of antibody-treated monkeys. As shown in **Figure 6**, the concentration of 3G8 reached a plateau at day 1, followed by a gradual decrease in both tamarins and cynomolgus monkeys, which was consistent with the kinetics of CD16$^+$ cells. In the case of MOPC-21 administration to tamarins, similar kinetics of its concentration with that of 3G8 were observed (data not shown).

### ATTENUATION OF CD16$^+$ NK CELL FUNCTION BY *IN VIVO* DEPLETION OF CD16$^+$ CELLS

Finally, we tested whether depletion of the CD16$^+$ subset could attenuate the NK activity in PBMCs. The killing activity was reduced at day 1 and the reduction persisted for 1 week post-treatment in the 3G8-treated monkeys (**Figure 7**). These results showed that the administration of the 3G8 mAb significantly influenced the number and activity of CD16$^+$ lymphocytes in both tamarins and cynomolgus monkeys.

## DISCUSSION

In this study, we attempted to establish a technical basis for the study of NK cells in tamarins. First, we characterized the NK cells in tamarins and showed that the anti-CD16 (3G8) mAb, an NK marker, cross-reacted with the PBMCs (**Figure 1**). Second, we assessed the killing activity of the CD16$^+$ NK cells in tamarins using our improved method (**Figures 2–4**) and demonstrated that CD16$^+$ NK cells were likely to be a major population with the killing activity in tamarins. Finally, to directly examine the role of CD16$^+$ NK cells *in vivo*, we assessed the effect of anti-CD16 (3G8) mAb *in vivo*. After administration of the mAb, CD16$^+$ NK cells were completely depleted and the killing activity was substantially attenuated in the treated monkeys (**Figures 5 and 7**). Our results suggest that our method for depletion of CD16$^+$ NK cells *in vivo* is useful for investigating the pivotal role of NK cells in the response against hepatitis viruses.

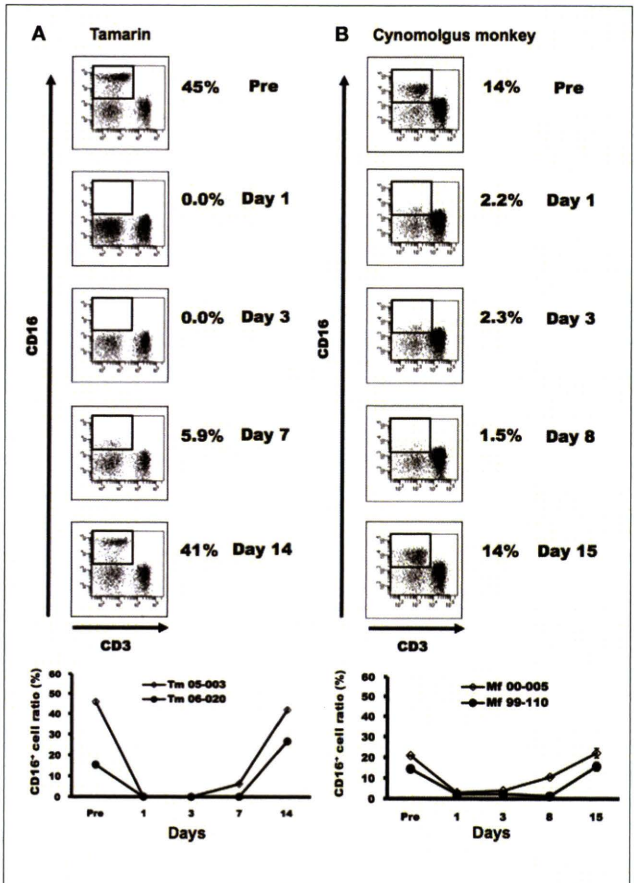


**FIGURE 5 | *In vivo* depletion of CD16$^+$ NK cells using a murine anti-CD16 (3G8) mAb in tamarins. (A,B)** Tamarins and cynomolgus monkeys were administered with 50 mg/kg of the 3G8 mAb. CD16$^+$ NK cell numbers were determined in whole blood specimens. Tamarins: Tm 05-003 and Tm 06-020. Cynomolgus monkeys: Mf 00-005 and Mf 99-110.

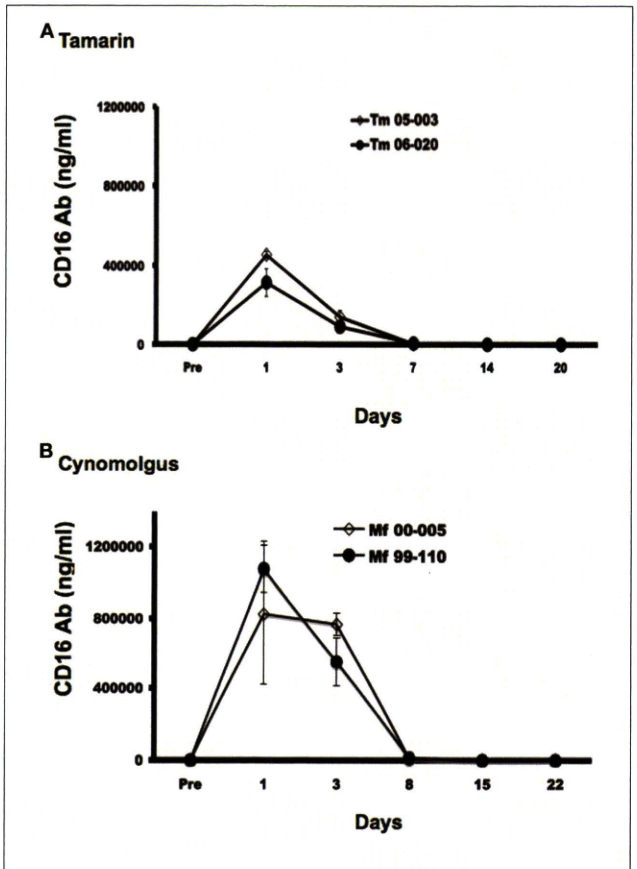


**FIGURE 6 | Kinetics of concentration of CD16 (3G8) mAb *in vivo*.** The concentration of CD16 (3G8) mAb in plasma was measured by ELISA as described in Section "Materials and Methods". Results shown are representative of three independent experiments. **(A)** Tamarins: Tm 05-003 and Tm 06-020. **(B)** Cynomolgus monkeys: Mf 00-005 and Mf 99-110.